Macromolecules **2002,** *35,* 5891−5902

Origin of Additional Mechanical Transitions in Multicomponent Polymeric Materials

D. Colombini and F. H. J. Maurer*

Department of Polymer Science & Engineering, Lund Institute of Technology, Center for Chemistry and Chemical Engineering, Lund University, P.O. Box 124 SE-22100 Lund, Sweden

Received February 19, 2002

ABSTRACT: The viscoelastic properties of several multicomponent materials (including both particulate multipolymeric materials and multilayer polymer blends) were investigated in relation to their microstructures and phase-property dependencies. Theoretical considerations based on mechanical modeling were used to explore the origin of additional mechanical transitions in experimental viscoelastic spectra. The major part of this work was devoted to particulate multicomponent systems, and especially to the further exploration of the characteristics of the so-called micromechanical transition (MMT). Although such an additional phenomenon is clearly explained as a result of a specific interphase, our investigation also provides evidence that the occurrence of a MMT in dynamic mechanical spectra reflects the contribution of the geometrical arrangement into phases of a set of properties of the pure components, rather than a molecular relaxational process within the interfacial area. Finally, on the basis of an equivalent approach, the influence of the geometrical arrangement of phases on the viscoelastic response of multilayer polymer blends was pointed out as a relevant argument to justify the existence of "spurious" additional damping peaks in some experimental dynamic mechanical spectra reported in the literature.

1. Introduction

The mechanical and viscoelastic properties of multiphase polymeric materials depend on molecular relaxation processes and morphology. Although these relaxations can usually be associated with each component, their appearance also depends on the chemical and physical interactions between the phases. These interactions may evolve in the existence of an interphase, whose thickness is inversely proportional[1] to the interfacial tension between the polymeric phases. Obviously, the properties of such an interfacial region differ from those of the pure components, and strongly affect the overall properties of the resulting blended material. As a consequence, an interphase must be considered to have a certain volume with its own characteristic properties or property gradients.

Although the concept of an interphase has been widely recognized, its in situ detection and characterization remain difficult. For this purpose, dynamic mechanical analysis (DMA) was proven to be an excellent method,[1−6] as this technique allows complete exploration of relaxational mechanisms in viscoelastic materials. By using compatibilizers,[1,2,4] specific interphases can be either previously introduced, or created in situ. In most cases, an interphase region leads to an additional damping peak in the dynamic mechanical spectra (DMS) of a multiphase polymeric system. Different hypotheses have been suggested to explain such an observation:

- a polymer layer having a higher stiffness than the bulk polymer in the vicinity of the dispersed phase surface is created from restricted molecular mobility due to interactions between phases,[5,7−11]
- a region close to the surface having a composition differing from the inclusion surface to the bulk matrix because of preferential adsorption of one of the components,[12]
- a region close to the surface having a different composition because of the incomplete dissolution of the fiber surface sizing in the reactive mixture of the matrix,[6]
- a layer close to the surface with different mechanical properties resulting from the residual thermal stresses, the adsorbed water, or the presence of voids.[13−14]

However, an additional damping peak in DMS does not necessarily reflect an interfacial relaxation process. On one hand, numerous examples of additional damping peaks have been reported[15−22] in the field of particulate multipolymeric systems. Thus, the viscoelastic properties of compatibilized poly(2,6-dimethyl-*p*-phenylene oxide) and poly(methyl methacrylate) (PPO/PMMA) blends were studied[15] by DMA. An interphase created by a minor addition of poly(styrene-graft-ethylene oxide) (P(SgEO)) copolymer was found to significantly change the dynamic mechanical behavior of these ternary blends of thermoplastics, and it was shown that the addition of the copolymer resulted in a new loss peak in the DMS of the blends. The new "transition" was theoretically presented[16−18] as a "micromechanical transition" (MMT), whose origin was explained by the change in the relative moduli values of the components in the matrix-interphase-particle structure of the blends, rather than by a molecular transition in any of the constituent. Other similar MMTs were also found[19] in $BaSO_4$-filled poly(styrene-*co*-acrylonitrile), as well as in compatibilized thermoset/thermoplastic blends.[20−22] Furthermore, in all cases,[15−22] Differential Scanning Calorimetry (DSC) measurements were also performed in their respective MMT temperature range, and no transitions were revealed.

On the other hand, several examples of unexpected additional damping peaks have been also reported[23−26] in the field of multilayer polymer blends. Thus, Nazarenko et al.[25] investigated several microlayer composites

---

* To whom correspondence should be addressed. Tel: (46) 46 222 91 49. Fax: (46) 46 222 41 15. E-mail: frans.maurer@polymer.lth.se.

10.1021/ma020266l CCC: $22.00

(with many alternating layers of poly(styrene-*co*-acrylonitrile) and polycarbonate), using DSC and DMA. They reported the observation of an additional transition, at a temperature between the glass transitions of the two components. The additional transition was observed in DMS but not in DSC scans, and its origin was explained[23] by assuming relative temperature dependencies of the controlling viscoelastic parameters over the appropriate temperature regimes. It was also considered[23,25] that such an anomalous peak could appear between the glass transition temperatures of the components when the modulus of the blended material cannot fall below the modulus of the glassy layers. Nazarenko et al.,[25] thus suggested that the intermediate damping peak was of purely mechanical origin, resulting from the mechanics of the anisotropic layered structure rather than the existence of a third phase. They concluded that such an observation could be considered a general feature of the dynamic mechanical behavior of co-continuous systems including polymer blends and continuous fiber composites. In addition to co-continuity of the phases, a large drop in modulus at the glass transition of the soft phase (i.e., with the lower glass transition temperature) was also required. McLaughlin[24] proposed a further refinement of the attribution of such a "spurious" loss transition (as defined by Gregory et al.[23]) related to the unique microstructure of continuous alternating sheets. Thus, McLaughlin correlated the intermediate tan δ transition with a microstructure composed of co-continuous phases in an alternating sheetlike arrangement.

The main objective of this work was to explore the origin of additional damping peaks in DMS of multicomponent materials, including both particulate multipolymeric materials and multilayer polymer blends. Theoretical considerations based on mechanical modeling have been used to provide evidence that specific geometrical arrangements can lead to additional loss damping peaks in DMS.

This paper will first focus on particulate multipolymeric systems in order to further explore the characteristics of the so-called MMT. In addition, some of the "spurious" loss transitions reported in multilayer polymer blends, will also be investigated with an equivalent approach.

2. Particulate Multipolymeric Materials

2.1. Theoretical Considerations − The Interlayer Model. Presentation. The prediction of the complex moduli of multiphase materials (polymer blends and composites) is usually based on phenomenological laws,[27] variational methods,[28−30] or self-consistent schemes[31−36] extended to describe viscoelastic behavior[16−19,22,37−43] through the correspondence principle.[44] Recently, the use of self-consistent mechanical models in *direct* and *reverse* modes was introduced.[22,37] The former leads,[16,17,22,37−42] as usual, to the prediction of the viscoelastic properties of a multicomponent system from the knowledge of the viscoelastic properties of all the pure components. The latter permits[22,37,41,43] the extraction of the actual viscoelastic characteristics of one phase blended among others in a heterogeneous polymeric system for specific morphologies. Both direct and reverse approaches are of interest for in-depth discussion[37] of the capability of the theoretical approach in the understanding of experimental dynamic mechanical data of complex polymeric materials.

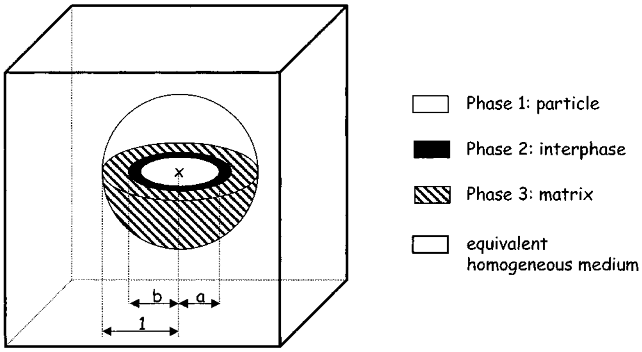

Figure 1. Illustration of a Representative Volume Element (RVE) of the interlayer model.

The interlayer model,[45−46] used in this work (in direct mode), represents an extension of van der Poel's theory,[47] which is closely connected to previous work[48] on the description of the viscosity of suspensions by a shell-model. To predict the dynamic mechanical shear properties of multipolymeric materials, the interlayer model requires the definition of a representative volume element (RVE). As depicted in Figure 1, such a RVE consists of three concentric spheres embedded in an equivalent homogeneous medium. The particle (Phase 1) is surrounded by a shell of interphase (Phase 2), which is covered by a shell of matrix (Phase 3). The radii of the spheres are chosen in accordance with the volume fractions of the different phases. In this way

$$V_1 = a^3,\ V_2 = b^3 - a^3,\ \text{and}\ V_3 = 1 - b^3 \tag{1}$$

Calculations are based on a set of common assumptions, which areas follows:

- linear elastic and viscoelastic behavior of phases,
- homogeneous and isotropic phases,
- continuity of displacements, radial and tangential stresses at the boundaries of the phases,
- no inertial forces,
- no defects, and,
- no thermal stresses.

On the basis of these boundary conditions, it is assumed that the response of the RVE to an external shear stress field is equal to the response of a volume element of homogeneous multipolymeric material.

Bulk Modulus. The external stress field applied to calculate the bulk modulus, K, of the homogeneous material is a hydrostatic pressure on its outer boundary. The general equations for displacements and stresses are solved by means of the continuity conditions on displacements or stresses at interfaces. Finally, according to the correspondence principle,[44] the complex bulk modulus, K*, is given by[45]

$$K^* = \frac{K_1^* V_1 + K_2^* V_2 R_k^* + K_3^* V_3 S_k^*}{V_1 + V_2 R_k^* + V_3 S_k^*} \tag{2}$$

with

$$R_k^* = \frac{3K_1^* + 4G_2^*}{3K_2^* + 4G_2^*} \tag{3}$$

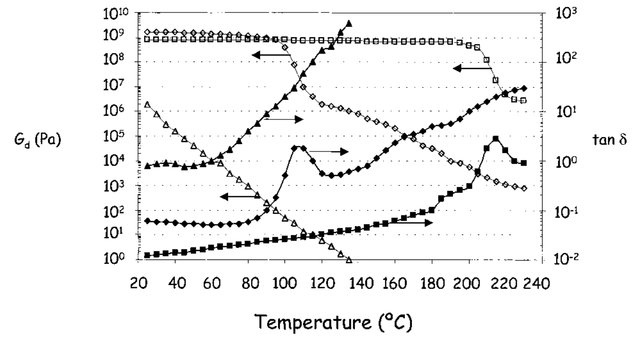

Figure 2. Viscoelastic characteristics, dynamic shear modulus (G_d) and loss factor (tan δ) at an angular frequency of 0.02321 rad·s^{-1}, versus temperature for pure components PMMA (♦ and ◊), PPO (■ and □), and P(SgEO) (▲ and △).

$$S_k^* = \frac{(3K_1^* + 4G_2^*)(3K_2^* + 4G_3^*) - 12d(K_2^* - K_1^*)(G_2^* - G_3^*)}{(3K_3^* + 4G_3^*)(3K_2^* + 4G_2^*)} \quad (4)$$

and

$$d = \frac{V_1}{V_1 + V_2} \quad (5)$$

Shear modulus. Analogous to the calculation of the bulk modulus, the complex shear modulus, G^*, is given by the solution of the following quadratic equation[45,46]

$$40\left[\frac{G^*}{G_3^*}\right]^2 |X^*| + \left[\frac{G^*}{G_3^*}\right]\{2|Y^*| + 8|Z^*|\} - 5|T^*| = 0 \quad (6)$$

where $|X^*|$, $|Y^*|$, $|Z^*|$, and $|T^*|$ are the determinants of the 10 × 10 submatrixes X^*, Y^*, Z^*, and T^*, defined in the Appendix.

2.2. Materials. To maintain a connection with previous experimental results,[15] our numerical simulations mainly concern polymer blends based on PMMA, PPO, and P(SgEO). Such a choice of multicomponent system is relevant, since it offers a comparison of both experimental and theoretical results. However, to further explore the viscoelastic characteristics of the MMT, several hypothetical multicomponent systems are also considered in the present study.

The overall viscoelastic behavior of pure components and PMMA/PPO/P(SgEO) blends were well characterized previously,[15] using a Rheometrics Analyzer RDA II in the oscillatory mode at an angular frequency of 0.02321 rad·s^{-1}. The viscoelastic characteristics of the pure components are shown in Figure 2. It can be observed that both PPO and PMMA show approximately constant moduli values up to their main α-relaxation (associated to their glass transition), leading to maxima of tan δ at 214 °C ($G''_{\max}$ *PPO* at 207 °C) and at 108 °C ($G''_{\max}$ *PMMA* at 100 °C), respectively. Although a weak, broad tan δ peak can be observed around 30 °C, the copolymer P(SgEO) behaves mainly like a polymer in the rubbery-liquid flow region. As a result, P(SgEO) has a much lower modulus than the other components, whose value always decreases with increasing temperature.

Furthermore, it was previously found[15] (Figure 3a) that the addition of P(SgEO) compatibilizer (from 1 to 10 volume parts) to PPO/PMMA (30/70 volume parts, respectively) blends resulted in a new loss peak in the DMS. The additional damping peak appeared in a distinctive temperature region of the ternary blends (from 50 °C to 90 °C, depending on the blend composition) and cannot be explained by a molecular transition in any of the pure components. Experimental data were then compared[16−18] to simulations, and this phenomenon was referred to a MMT to distinguish it from other ordinary molecular transitions. The temperature at which the MMT occurred in DMS was predicted to depend on the volume fraction (Figure 3b) and on the Poisson ratio (Figure 3c) of the interphase component.

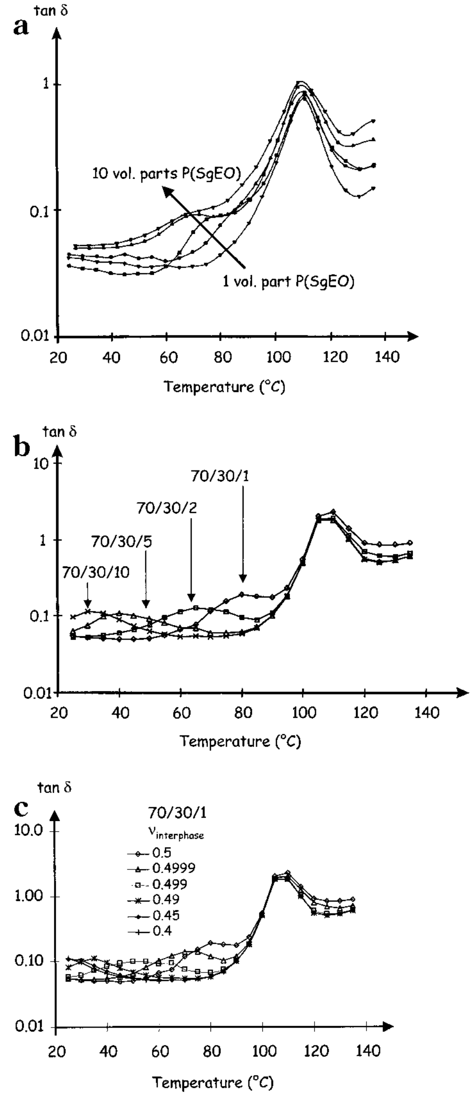

Figure 3. Experimental and theoretical evolution of the loss factor, tan δ, versus temperature for PMMA/PPO/P(SgEO) blend. (a) Experimental influence of the blend composition, from Eklind et al.[15] (b) Theoretical influence of the blend composition (ν = 0.5 for all the components). (c) Theoretical influence of the Poisson ratio ν of the interphase component (blend composition 70/30/1). *These theoretical results were obtained on the basis of previous investigations* [16]. *The blend compositions are given in volume parts of matrix/particle/interphase.*

2.3. Numerical Results and Discussion. Earlier, MMT was explained[16−18] by the change in the relative values of the moduli of the components in the matrix-interphase-particle structure of a multicomponent system. Such a description would suggest the following primary questions:

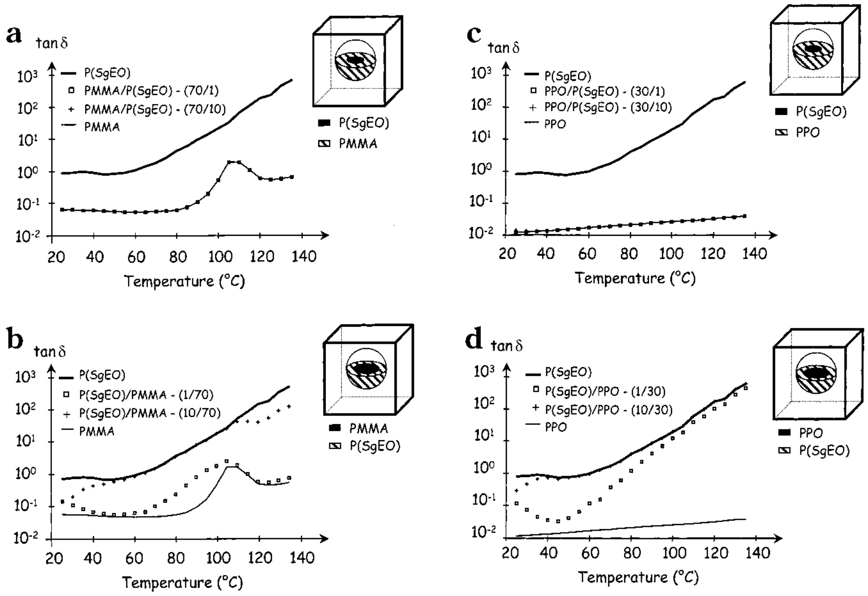

Figure 4. Theoretical loss factor tan δ versus temperature for binary blends (compositions given in volume parts of each component). (a) Matrix: PMMA – particle: P(SgEO). (b) Matrix: P(SgEO) – particle: PMMA. (c) Matrix: PPO – particle: P(SgEO). (d) Matrix: P(SgEO) – particle: PPO. *The experimental viscoelastic behavior for pure components is presented for comparison.*

- Can we observe a MMT in DMS of a multipolymeric material that does not contain a significant interphase?
- Is the change in the relative values of the moduli of the components, a necessary condition for the observation of a MMT in DMS?
- Are these two conditions (i.e., the presence of both an interphase and a change in the relative moduli of components) sufficient for the observation of a MMT in DMS?

In the following section, we will attempt to answer the above questions, to point out the role of the morphology before further exploring the phase-property-dependence of a MMT.

2.3.1. Primary Questions Based on the First Descriptions of MMT in Multipolymeric Materials. Can we Observe a MMT in DMS of a Multipolymeric Material that does not Contain a Significant Interphase? From a theoretical point of view, it is easy to perform numerical simulations by assuming a volume fraction of interphase equal to zero. We considered binary blends based on P(SgEO) (1 or 10 vol. parts), and PMMA (70 vol. parts) or PPO (30 vol. parts). Figure 4 shows the theoretical results for such P(SgEO)/PMMA (Figure 4a and 4b) and P(SgEO)/PPO binary systems (Figure 4c and 4d), where each component was successively considered either as the matrix or as the particle.

First, it can be observed in all of these plots that whatever the binary system or its composition, the overall prediction of the loss factor, tan δ, essentially follows that of the chosen continuous phase. Such an observation is in agreement with Bohn's conclusions,[49] related to the main influence of the continuous phase on the viscoelastic properties of a polymer blend. But the most important point here is that no additional damping peak was predicted in the temperature range from 50 °C to 90 °C, whatever the numerical simulation.

As a consequence, the presence of an interphase that has to be defined as a topological entity separated by two phases (i.e., a phase between two phases), must be considered necessary to observe a MMT in DMS.

Is the Change in the Relative Values of the Moduli of the Components an Indispensable Condition for the Observation of a MMT in DMS? As illustrated in Figure 2, the dynamic shear modulus of the interphase component (P(SgEO)) gradually decreases over the whole temperature range investigated. At the same time, both matrix (PMMA) and particles (PPO) show almost constant moduli between room temperature and 90 °C. To investigate the importance of such a change in the relative values of the moduli of the components regarding the observation of a MMT in DMS, we used the interlayer model to predict the viscoelastic properties of several hypothetical blends. To maintain a connection with the PMMA/PPO/P(SgEO) system, the properties of the matrix component ($G_d^{matrix} = 1.6 \times 10^9$Pa, tan $\delta_{matrix} = 0$, $\nu_{matrix} = 0.33$) as well as those of the spherical particles ($G_d^{particle} = 0.8 \times 10^9$Pa, tan $\delta_{particle} = 0$, $\nu_{particle} = 0.33$) were defined as constant in these numerical calculations. Concerning the viscoelastic properties of the interphase component, a preliminary series of simulations was performed for matrix/particle/interphase 70/30/x (x = 1, 2, 5, 10) blends also assuming constant interphase properties ($G_d^{interphase} = 2 \times 10^6$Pa or 200Pa, $\nu_{interphase} = 0.5$, tan $\delta_{interphase} \in \{0.1; 1; 10; 100\}$). However, no additional damping peaks were observed for any of the cases where no change in the relative values of the moduli was considered in the numerical simulations.

In addition to these preliminary numerical results, other calculations were performed assuming a significant variation in the dynamic shear modulus of the interphase component ($G_d^{interphase}$ varying from 10^7 to 1Pa, tan $\delta_{interphase} = 1$, $\nu_{interphase} = 0.5$). It should be noted that such a series of input data is very similar to that for the PMMA/PPO/P(SgEO) ternary polymer blend. The results of the numerical simulations are shown in Figure 5. Figure 5a presents the calculated quotients of the dynamic shear modulus of the blend and either that of the matrix or that of the particle, and Figure 5b shows the corresponding loss factor, tan δ, for the hypothetical matrix/particle/interphase 70/30/x (where x is 1, 2, 5, or 10 volume parts). These data are given as a function of the dynamic shear modulus of the interphase component in Figure 6a and 6b.

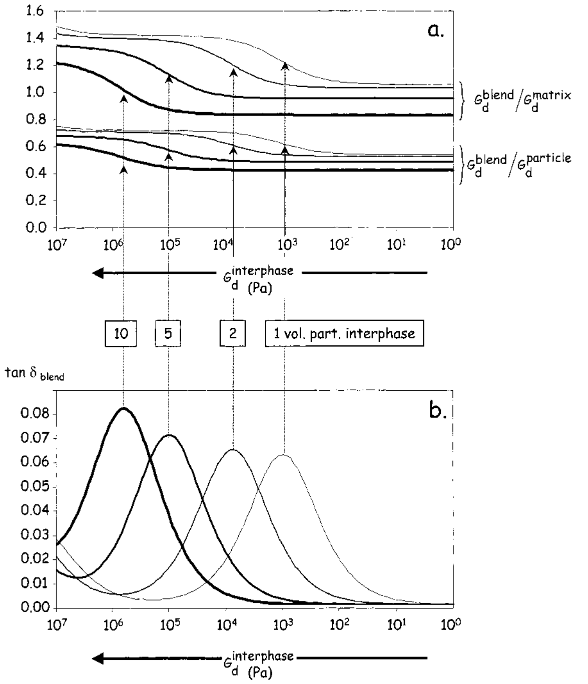

Figure 5. Modeling of the viscoelastic properties of theoretical matrix/particle/interphase (70/30/x vol. parts, where $x = 1$, 2, 5, or 10) blends. (a) ($G_\mathrm{d}^\mathrm{interphase}/G_\mathrm{d}^\mathrm{matrix}$) and ($G_\mathrm{d}^\mathrm{interphase}/G_\mathrm{d}^\mathrm{particle}$) versus $G_\mathrm{d}^\mathrm{interphase}$. (b) Loss factor tan δ versus $G_\mathrm{d}^\mathrm{interphase}$.

As indicated by vertical arrows (Figure 5) for each blend, both relative moduli drop from a higher to a lower level, as tan δ shows a maximum. The magnitude of the additional damping peak is also related to the slope of the change in the relative moduli. Thus, the more significant the slope, the higher the value at the maximum of tan δ. Furthermore, the position and magnitude of the fall in the moduli ratios (Figure 5a), as well as the maximum of tan δ (Figure 5b), occur at higher interphase modulus values with increasing volume fraction of the interphase. As tan δ was defined to be constant for each component in the hypothetical blends, such a predicted maximum of tan δ is related to the change in the relative moduli of the components, since only the modulus of the interphase was varied in the numerical simulations.

As a preliminary answer to our primary questions, both a topological interphase and relative values of the moduli of the components appear to be necessary conditions for the observation of a MMT in DMS.

Are these Two Conditions Sufficient for the Observation of a MMT in DMS? Behind the question of the sufficiency of the above-mentioned necessary conditions lies mainly the importance of the geometrical arrangement of the different phases (so-considered morphology in the mechanical model) in the observation (or not) of a MMT in DMS. If these two conditions are sufficient then, for a given system leading to a MMT, the additional damping peak should be predicted by the interlayer model whatever the geometrical arrangement. The ternary blend PMMA/PPO/P(SgEO) 70/30/5 was chosen for such an investigation. Figure 3b shows that the evolution of the predicted loss factor, tan δ, leads to a MMT at around 45 °C, when P(SgEO) is considered as interphase component. This result is included in Figure 6, which also shows the theoretical evolution of the loss factor, tan δ, obtained using exactly the same input data (i.e., properties and volume fractions of pure components) where PPO was considered as interphase instead of P(SgEO). It can be seen that the additional damping peak is only predicted when P(SgEO) was considered as the interphase component. Such a result underlines the importance of the microstructure for the observation of a MMT in DMS.

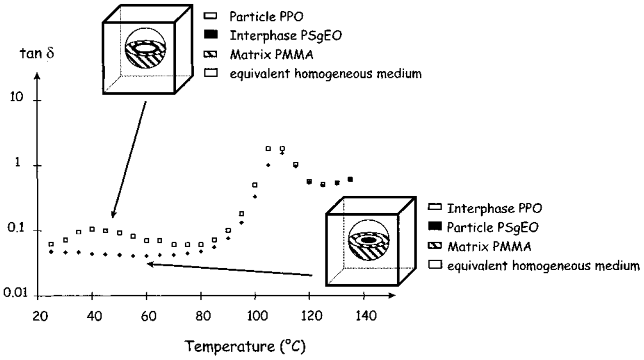

Figure 6. Theoretical viscoelastic properties of PMMA/PPO/P(SgEO) (70/30/5) blends considering P(SgEO) as either the interphase component or as the dispersed phase.

As a consequence, the presence of both an interphase and a change in the relative moduli of the components have been shown to be necessary conditions but not sufficient. An MMT is therefore not the sole result of a particular set of properties of the pure components of a multipolymeric system. Instead, it can be considered that the observation of a MMT is a strong indication of the presence of a interphase component (surrounding inclusions), whose properties affect the overall relative moduli of blended material and component.

2.3.2. Further Exploration of both Phase-Property-Dependence and the Characteristics of the MMT. The study of the influence of the blend composition on the predicted viscoelastic characteristics of MMT in DMS for the PMMA/PPO/P(SgEO) system has been described in detail previously.[16] As recalled in Figure 3b, a significant influence of the volume fraction of the interphase on the temperature location of the MMT was reported.[16] In the following section, we will focus on the theoretical influence of the phase properties (i.e., the dynamic shear moduli and Poisson ratios) and blend composition on the viscoelastic characteristics (i.e., temperature location, magnitude, and width) of a MMT in DMS. As a consequence of the observations described in the previous section, the influence of the properties of the interphase component will take up most of our attention, whereas those of the matrix and particle will be only briefly discussed.

Theoretical Influence of the Poisson Ratio of the Components. The influence of the Poisson ratio, ν, of the matrix, particle and interphase on the overall viscoelastic response of the PMMA/PPO/P(SgEO) blend was studied theoretically for two blend compositions (70/30/1 and 70/30/5). First, the influence of ν for both matrix (PMMA) and particle (PPO) was investigated. The Poisson ratio of the interphase component was fixed at 0.5, whereas several constant values (in the range from 0.33 to 0.5) were selected for the other components. Numerical simulations were performed for three different cases: $\nu_\mathrm{particle} < \nu_\mathrm{matrix}$ (Figure 7a), $\nu_\mathrm{particle} > \nu_\mathrm{matrix}$ (Figure 7b), and $\nu_\mathrm{particle} = \nu_\mathrm{matrix}$ (Figure 7c). As can be seen in Figure 7, for a given blend composition, all predicted evolutions of the loss factor, tan δ, are superimposed, regardless of the values of ν_matrix and ν_particle. In consequence, it can be concluded that the

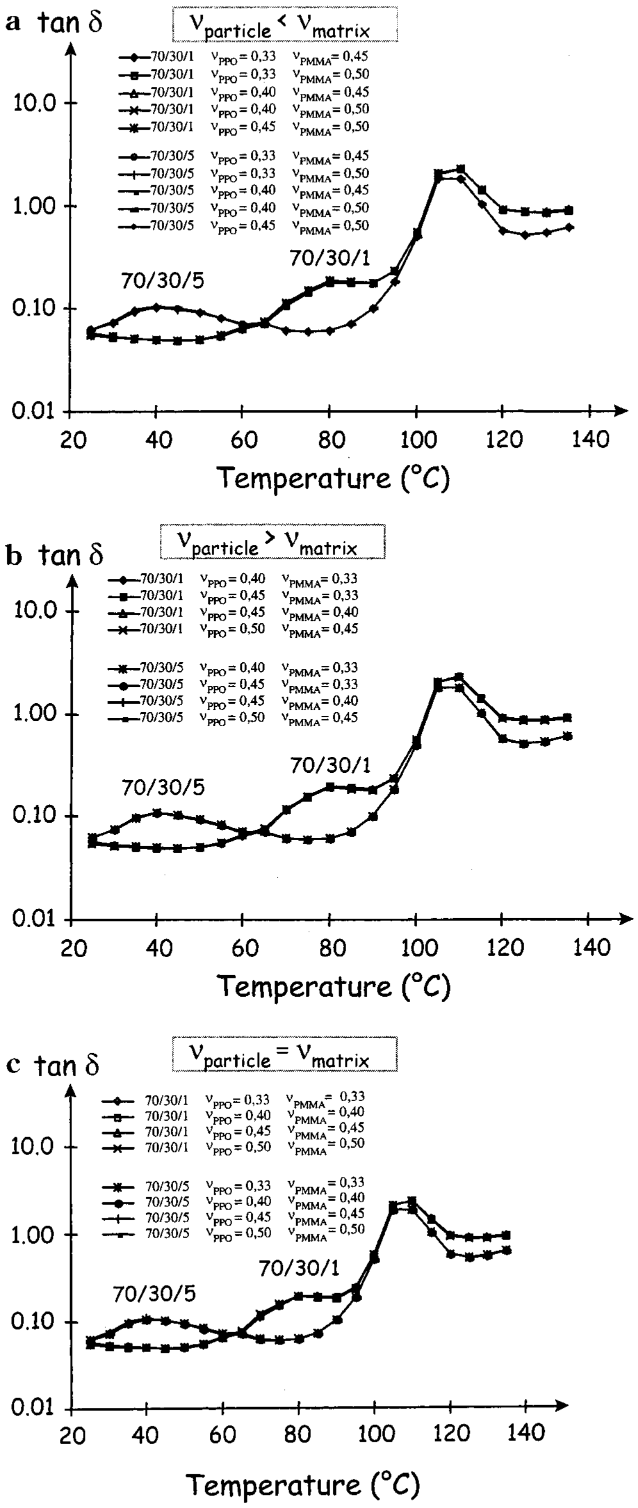

Figure 7. Influence of the Poisson ratios, ν, of both matrix (PMMA) and particle (PPO) on the evolution of the predicted loss factor, tan δ, versus temperature. (a) $\nu_{\text{particle}} < \nu_{\text{matrix}}$; (b) $\nu_{\text{particle}} > \nu_{\text{matrix}}$; (c) $\nu_{\text{particle}} = \nu_{\text{matrix}}$.

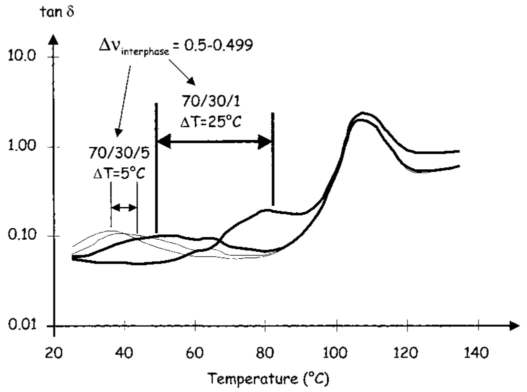

Figure 8. Composition dependence of the theoretical influence of the Poisson's ratio of the interphase component.

compressibility of both the matrix and the particle have no significant influence on the overall viscoelastic response of the ternary system in this temperature range.

In contrast, Figure 3c reveals that, for the 70/30/1 composition, the response is highly dependent on the Poisson ratio of the interphase component.[16] It can be seen that the position of the MMT is shifted by about 25 °C toward lower temperatures as $\nu_{\text{interphase}}$ changes from 0.5 to 0.499. Such an amazing observation is, however, dependent on the volume fraction of the interphase. As shown in Figure 8, for the same $\Delta\nu_{\text{interphase}}$ (variation from 0.5 to 0.499), the temperature location of the MMT is shifted approximately 5 °C toward lower temperatures when the blend composition is 70/30/5 instead of 70/30/1. In any cases, such a noticeable influence of $\nu_{\text{interphase}}$ strongly indicates that the compressibility of the interfacial area in a polymer blend substantially affects the overall viscoelastic response of the multicomponent system.

Obviously, this theoretical result is very difficult to confirm experimentally. However, a MMT was studied in detail[20] in a compatibilized thermoset/thermoplastic blend. It was found experimentally that the magnitude and the temperature location of the MMT in DMS were strongly dependent on the thermal history of the samples. Several thermal treatments were applied, and it was suggested that the viscoelastic behavior of the ternary polymer blend could be directly associated with the expansion of the components. Such an interpretation was then confirmed by another study[50] based on molecular dynamics (MD) simulations, where both the structure and the mobility (at the molecular level) of an interphase component were studied in response to a volume expansion such as might occur in actual systems. From a general point of view, the effects of volume expansion are reasonably expected to be higher when the amount of interphase in the material is lower. On this basis, experimental[20] and MD[50] results can support the differences in shifting of temperature location such as those seen in Figure 8 after changing the blend composition.

Theoretical Influence of the Viscoelastic Properties of the Components. To further explore the interphase-property-dependence of MMT in DMS, it is now relevant to perform numerical simulations in the frequency domain by considering an angular shift (α) of the dynamic shear modulus of the interphase component. To properly investigate the theoretical influence of such an angular shift of $G_{\text{d}}^{\text{interphase}}$, isothermal input data were used over a wide frequency range. As a matter of fact, both the phase angle, δ, and G_{d} are frequency (ω) and temperature (T) dependent quantities, and the two quantities are directly related to each other by the following relationship[51]

$$\delta(\omega,T) \approx \frac{\pi}{2}\left|\frac{\partial\ \text{Log}\ G_{\text{d}}(\omega_i,\ \text{T})}{\partial\ \text{Log}\ \omega_i}\right|_{\omega_i} \qquad (7)$$

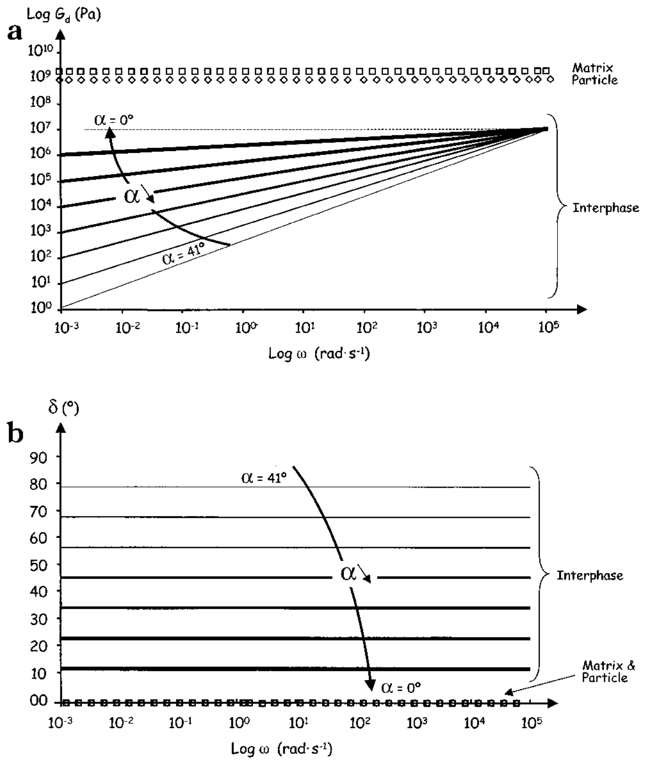

Figure 9. Viscoelastic input data used to study the influence of an angular shift (α) of the dynamic shear modulus of the interphase component. (a) G_d versus frequency. (b) Resulting tan δ versus frequency. *The evolution of the angle α is highlighted by the arrow.*

The input data used to perform the numerical simulations are shown in Figure 9 and obey relation (7). The angular shift (α) is defined (Figure 9a) as the angle between the dashed line at $G_d^{\text{interphase}}$ equal to 10^7Pa (α = 0°) and the variation of $G_d^{\text{interphase}}$ (from 10^7 to 10^x with $x \in [0;6]$) considered in the simulations. To make comparison with the above results easier, the following hypothetical blends were chosen:

- Matrix: 70 volume parts, $G_d^{\text{matrix}} = 1.6 \times 10^9$Pa, tan $\delta_{\text{matrix}} = 0$, $\nu_{\text{matrix}} = 0.33$
- Particle: 30 volume parts, $G_d^{\text{particle}} = 0.8 \times 10^9$Pa, tan $\delta_{\text{particle}} = 0$, $\nu_{\text{particle}} = 0.33$
- Interphase: 1 or 5 volume parts, ($G_d^{\text{interphase}}$, $\delta_{\text{interphase}}$) as defined in Figure 9, $\nu_{\text{interphase}} = 0.5$ or 0.499

Figure 10 shows the theoretical results obtained for a 70/30/5 hypothetical blend with $\nu_{\text{interphase}} = 0.5$. For the entire angular shift range, predicted values of both G_d and tan δ are given versus frequency. As expected, all the theoretical evolutions of the loss factor present a MMT damping peak. At the same time as tan δ shows a maximum, G_d drops from a lower level to a higher. When α decreases, it can be noticed that:

- the width of the tan δ peak increases,
- the magnitude of the tan δ peak decreases,
- and the frequency location of the maximum is shifted toward lower frequencies.

Obviously, the areas under the damping curves remain almost constant, since the predicted drops of G_d are almost similar.

It was then also deemed to be of interest to investigate how a change in either the volume fraction or the Poisson ratio of the interphase component could affect the theoretical curves given in Figure 10. Figure 11 shows the results of such an investigation. First, it can be observed that all cases exhibit the same tendency as that presented in Figure 10. However, when the amount of interphase decreases (Figures a→c, or b→d), a significant shift of the frequency location of the MMT toward lower frequencies is observed. At the same time, the magnitude of the damping peak decreases. Furthermore, when $\nu_{\text{interphase}}$ decreases slightly from 0.5 to 0.499, a significant shift in the frequency locations of the MMT toward higher frequencies is observed, whereas the magnitudes remain unchanged.

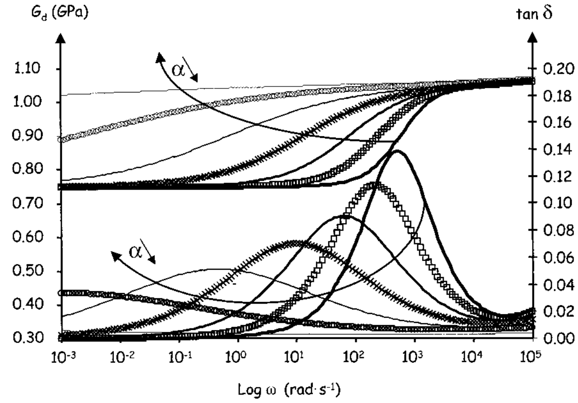

Figure 10. Predicted viscoelastic properties (dynamic shear modulus, G_d , and loss factor, tan δ) for a matrix (70 vol. parts; $\nu = 0.33$)/particle (30 vol. parts; $\nu = 0.33$)/interphase (5 vol. parts; $\nu = 0.5$) blend versus frequency as a function of the angular shift α of $G_d^{\text{interphase}}$. *The evolution of the angle α is indicated by the arrows.*

As already pointed out in Figure 8, such a reduction of $\nu_{\text{interphase}}$ (from 0.5 to 0.499) is more important when the amount of interphase is lower. This point is perfectly highlighted in Figure 12, which shows results obtained with the same set of viscoelastic properties of pure hypothetical components (α = 41° for the interphase).

As a result of our further exploration of such an additional damping peak, so-called micromechanical transition and denoted MMT, it is concluded that:

- An MMT is different from classical molecular transitions, which solely reflect the molecular relaxation of macromolecules.
- The observation of such a phenomenon requires the presence of a specific interphase, whose properties affect the overall relative moduli of the blended material and its components.
- The observation of a MMT in DMS of multicomponent systems must be interpreted as an indicator of the manifestation of its interfacial area, the compressibility of which strongly influences the viscoelastic characteristics of the MMT.
- However, even if a MMT results from the contribution of the interphase properties to the overall relative moduli, its occurrence in DMS reflects the geometrical arrangement into phases of a set of properties of pure components, rather than molecular or macromolecular relaxational process within the interfacial area.
- In this context, the concept of interphase must be considered as a topological entity separated by two other phases. Such precision does not restrict the observation of a MMT to the sole field of particulate multipolymeric systems, which are the only ones to present a particle-interphase-matrix structure: as a result, such an additional damping peak could also be found in multilayer polymer blends or composites.

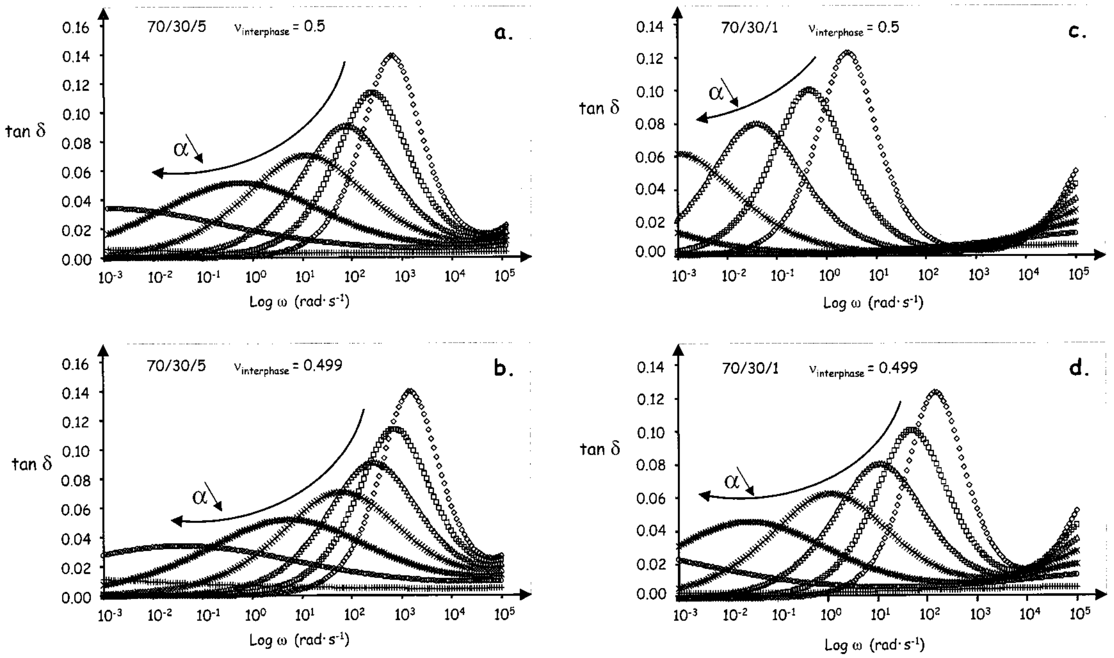

Figure 11. Influence of the angular shift, α, of $G_d^{\mathrm{interphase}}$ on the theoretical viscoelastic properties of blends. (a) 70/30/5 (vol. parts) and $\nu_{\mathrm{interphase}} = 0.5$. (b) 70/30/5 (vol. parts) and $\nu_{\mathrm{interphase}} = 0.499$. (c) 70/30/1 (vol. parts) and $\nu_{\mathrm{interphase}} = 0.5$. (d) 70/30/1 (vol. parts) and $\nu_{\mathrm{interphase}} = 0.499$. *The evolution of the angle α is indicated by the arrows.*

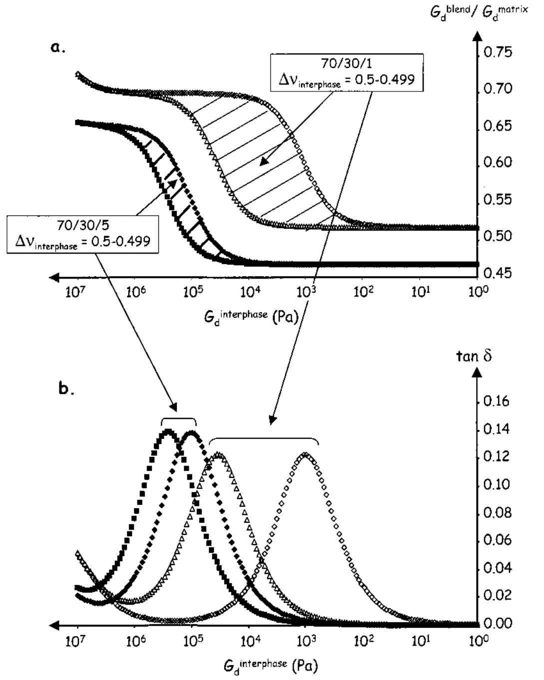

Figure 12. Composition dependence of the theoretical influence of $\nu_{\mathrm{interphase}}$ (α = 41°).

3. Multilayer Polymer Blends

In the field of multilayer polymer blends, numerous observations of unexpected additional transitions have been reported.[23-26] All of these microlayer composites were based on many alternating layers of two polymers, whose glass transition temperatures were significantly different. In all cases, a third damping peak was observed at a temperature intermediate to the damping peaks corresponding to the glass transitions of the two components.

3.1. Theoretical Considerations. On one hand, the complex moduli of a multilayer polymer blend can be predicted by using the well-known parallel mechanical combination of elements, the so-called "parallel model".[28] As a result of isostrain conditions, and according to the correspondence principle,[44] the complex shear modulus, G^*, of a multilayer blend of polymer A and polymer B is given by

$$G^* = V_A \cdot G_A^* + V_B \cdot G_B^* \tag{8}$$

where G_A^*, and G_B^* are the complex shear modulus of pure constituents A and B, respectively, and V_A, and V_B are the volume fractions of the pure constituents.

On the other hand, theoretical predictions based on the interlayer model can also be taken into consideration. Such an investigation will require the definition of a representative volume element (RVE, as depicted in Figure 1), in which one polymer is considered as particle and matrix (i.e., phases 1 and 3, respectively) whereas, at the same time, the other acts as interfacial layer (phase 2).

3.2. Hypothetical Materials. To maintain a connection with previous investigations,[23-26] two hypothetical amorphous polymers A and B, with a large difference in their glass transition temperatures, were considered in our numerical simulations. The viscoelastic properties of polymer A were chosen from the glassy state to the rubbery-liquid flow region (as shown in Figure 13), whereas polymer B was considered to be in the glassy state with constant viscoelastic properties ($G_d = 0.8 \times 10^9$Pa, tan $\delta = 10^{-4}$) over the whole temperature range considered.

3.3. Numerical Results and Discussion. As depicted in the top right-hand corner of Figure 14, the parallel model was first used to perform numerical simulations based on A/B multilayer polymer blends, in the composition range from 40/60 to 60/40 (A/B volume parts). First of all, the presence of the maximum of tan δ, corresponding to the main relaxation of polymer A, can be observed at about 100 °C. The slight change in the temperature location of the maximum of

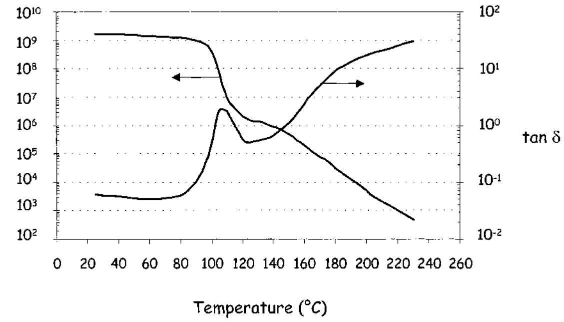

Figure 13. Viscoelastic input data used for polymer A: G_d and tan δ versus temperature.

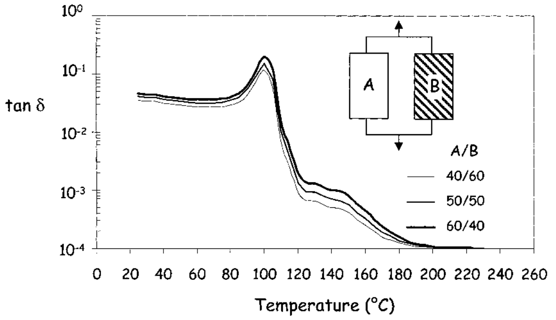

Figure 14. Theoretical loss factor, tan δ, versus temperature, as predicted by the parallel model, for the hypothetical multilayer A/B polymer blend. *The blend compositions are indicated in volume parts of each component.*

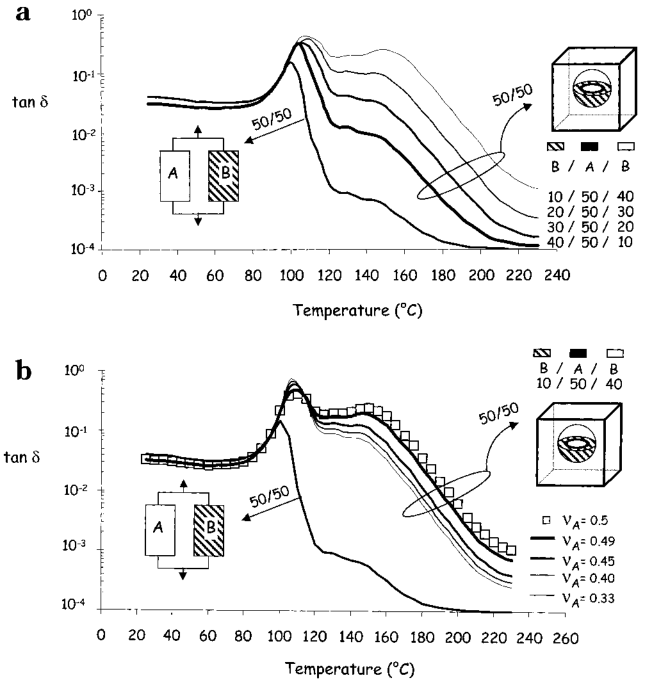

Figure 15. Theoretical loss factor, tan δ, versus temperature, as predicted by the interlayer model, for the hypothetical multilayer A/B polymer blend (50/50). (a) Influence of the interphase thickness ($\nu_A = \nu_B = 0.5$). (b) Influence of $\nu_{\text{interphase}}$ (ν_A). *The blend compositions B/A/B are indicated in volume parts of matrix/interphase/particle, respectively. The theoretical prediction by the parallel model is shown for comparison.*

tan δ, compared to that of pure polymer A (Figure 13), reflects[42,49] the mechanical coupling effects between phases in the A/B system. Furthermore, as a result of the association of the properties of both components, Figure 14 also reveals the presence of a weak additional peak in tan δ around 140 °C, the intensity of which increases with the amount of polymer A. Because such a mechanical transition is not present in any of the constituent materials A and B, its origin must be found in the relative change of moduli caused by the gradual decrease of polymer A from the rubbery plateau into the liquid-flow region.

The question arises as to whether a change in the geometrical arrangement of phases A and B results in similar effects on the overall theoretical viscoelastic blend properties predicted by the interlayer model. Numerical simulations based on a RVE with a layer of polymer A (phase 2) between two layers of polymer B (phases 1 and 3) were therefore performed. As a given binary blend composition (A/B) can lead to several combinations of the volume fractions V_1 and V_3 (with $V_1 + V_3 = V_B$), our calculations were only performed for the 50/50 blend composition.

Figure 15a presents the numerical results obtained by assuming constant Poisson ratios ($\nu_A = \nu_B = 0.5$), a constant amount of interphase ($V_A = 50$ volume parts) and several sets of values (indicated in Figure 15a) for the volume parts of particle and matrix, both based on polymer B. First, it can be seen in Figure 15a that the main relaxation of polymer A occurs at almost the same temperature location as the pure constituent (Figure 13). Just as in simulations based on the parallel model (Figure 14), an additional mechanical transition is also predicted at a temperature in the range 140 °C-160 °C. It is important to notice that, for the same A/B blend composition (50/50), the temperature location as well as the magnitude of the additional transition increase when the matrix (B) / interphase (A) / particle (B) blend distribution is changed from 40/50/10 to 10/50/40. Such an observation is consistent with our previous discussion (section 2.3.2) in the case of particulate multipolymeric materials.

The influence of the Poisson ratio of the components A and B on the theoretical viscoelastic response of the B/A/B blend was also investigated. In the first series of calculations, the Poisson ratio of the interphase (ν_A) was kept constant at 0.5, whereas several constant values (from 0.33 to 0.5) were chosen for ν_B. In agreement with the results in Figure 7, the overall theoretical viscoelastic response was found not to be affected by such a change in the compressibility of polymer B. On the other hand, for the 10/50/40 blend composition, Figure 15b shows that this response is dependent on the Poisson ratio of the interphase component, ν_A. As a matter of fact, the additional transition is found to be shifted toward lower temperatures (and decreased in magnitude) as ν_A decreases from 0.5 to 0.33.

Figures 8 and 12 showed that the influence of a small change $\Delta\nu_{\text{interphase}}$ was more important for a small amount of interphase. Similarly, Figure 16 shows the numerical results obtained by considering the same amount of interphase ($V_A = 50$ vol. parts), the same variation $\Delta\nu_{\text{interphase}}$ (from 0.5 to 0.33), and the same overall blend composition (50/50). It should be noted that the sole difference in these calculations lies in the geometrical arrangement of the phases (40/50/10 and 10/50/40, respectively). It should be especially observed that the changes in magnitude and temperature location of the additional transition are more noticeable when the geometrical matrix/interphase/particle phase repartition is 10/50/40. Thus, in addition to Figure 8 and Figure 12 concerning simulations based on particulate multipolymeric systems, Figure 16 shows that, at a

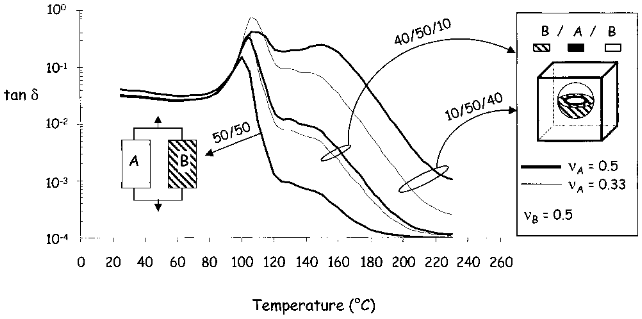

Figure 16. Composition dependence of the theoretical influence of $\nu_{\mathrm{interphase}}$ for the hypothetical multilayer A/B polymer blend.

constant amount of interphase, the influence of the compressibility of the interphase is even more important when the volume fraction of the occlusion increases. From a practical point of view, these last arguments are sufficient to justify the observation of "unexpected" additional damping peaks in some experimental dynamic mechanical spectra of multilayer polymer blends.

4. Conclusion

In this study, the interlayer model was used to explore the origin of additional damping peaks that were observed in DMS but not in DSC scans of multicomponent polymeric materials.

By first mainly focusing on particulate multipolymeric systems, a detailed discussion of the so-called micromechanical transition was performed. The importance of both microstructure (or geometrical arrangement of phases) and phase-property-dependence on the viscoelastic characteristics of a MMT in DMS was especially emphasized. The interphase component, with its own properties and specific contribution to the overall relative viscoelastic behavior of the blended systems, was found to play a crucial role in the occurrence of MMT in DMS. Although such a phenomenon was clearly identified as a result of a specific interphase (so-considered as a topological entity between two phases, whose interfacial properties strongly affect the overall relative moduli of the multipolymeric material and its components), it was found that the occurrence of a MMT in DMS reflects the contribution of the geometrical arrangement into phases of a set of properties of pure components, rather than molecular relaxational process within the interfacial area.

A similar approach was then used to investigate multilayer polymer blends. Based on both parallel and interlayer models, our theoretical predictions led to arguments relevant for the understanding of the additional damping phenomena observable in dynamic mechanical experiments.

Appendix

The complex shear modulus, G^*, is given by the solution of the following quadratic equation

$$40\left[\frac{G^*}{G_3^*}\right]^2|X^*| + \left[\frac{G^*}{G_3^*}\right]\{2|Y^*| + 8|Z^*|\} - 5|T^*| = 0$$

where the determinants $|X^*|$, $|Y^*|$, $|Z^*|$, and $|T^*|$ are given below as functions of the volume fractions (V_i) and the Poisson ratios (ν_i) of each phase i (where i = 1, 2, or 3, as described in Figure 1).

The quotient of the shear modulus of the filler (G_1^*) and the shear modulus of the layer (G_2^*) is defined by M. The quotient of the shear modulus of the layer (G_2^*) and the shear modulus of the matrix (G_3^*) is defined by P. Thus

$$M = \frac{G_1^*}{G_2^*} \text{ and } P = \frac{G_2^*}{G_3^*}$$

Field Elements of the Submatrix $|X^*|$. (The Elements not Listed have the Value Zero.)

$$X[1,1] = X[2,1] = M$$

$$X[1,2] = -\frac{1}{2}MV_1^{2/3}$$

$$X[1,3] = -1$$

$$X[1,4] = 4V_1^{-5/3}$$

$$X[1,5] = \frac{1}{2}V_1^{2/3}$$

$$X[1,6] = V_1^{-1}\left(\frac{10 - 2\nu_2}{5 - 4\nu_2}\right)$$

$$X[2,2] = MV_1^{2/3}\left(\frac{7 + 2\nu_1}{6\nu_1}\right)$$

$$X[2,3] = -1$$

$$X[2,4] = -\frac{8}{3}V_1^{-5/3}$$

$$X[2,5] = -V_1^{2/3}\left(\frac{7 + 2\nu_2}{6\nu_2}\right)$$

$$X[2,6] = -V_1^{-1}\left(\frac{2 + 2\nu_2}{5 - 4\nu_2}\right)$$

$$X[3,1] = V_1^{1/3}$$

$$X[3,2] = V_1$$

$$X[3,3] = -V_1^{1/3}$$

$$X[3,4] = -V_1^{-4/3}$$

$$X[3,5] = -V_1$$

$$X[3,6] = -V_1^{-2/3}$$

$$X[4,1] = \frac{1}{2}V_1^{1/3}$$

$$X[4,2] = V_1\left(\frac{7 - 4\nu_1}{12\nu_1}\right)$$

$$X[4,3] = -\frac{1}{2}V_1^{1/3}$$

$$X[4,4] = \frac{1}{3}V_1^{-4/3}$$

$$X[4,5] = -V_1\left(\frac{7 - 4\nu_2}{12\nu_2}\right)$$

$$X[4,6] = -\,V_1^{-2/3}\left(\frac{1-2\nu_2}{5-4\nu_2}\right)$$

$$X[5,3] = P$$

$$X[5,4] = -4P(V_1 + V_2)^{-5/3}$$

$$X[5,5] = -\frac{1}{2}P(V_1 + V_2)^{2/3}$$

$$X[5,6] = -P(V_1 + V_2)^{-1}\left(\frac{10-2\nu_2}{5-4\nu_2}\right)$$

$$X[5,7] = -1$$

$$X[5,8] = 4(V_1 + V_2)^{-5/3}$$

$$X[5,9] = \frac{1}{2}(V_1 + V_2)^{2/3}$$

$$X[5,10] = (V_1 + V_2)^{-1}\left(\frac{10-2\nu_3}{5-4\nu_3}\right)$$

$$X[6,3] = P$$

$$X[6,4] = \frac{8}{3}P(V_1 + V_2)^{-5/3}$$

$$X[6,5] = (V_1 + V_2)^{2/3}P\left(\frac{7+2\nu_2}{6\nu_2}\right)$$

$$X[6,6] = (V_1 + V_2)^{-1}P\left(\frac{2+2\nu_2}{5-4\nu_2}\right)$$

$$X[6,7] = -1$$

$$X[6,8] = -\frac{8}{3}(V_1 + V_2)^{-5/3}$$

$$X[6,9] = -(V_1 + V_2)^{2/3}\left(\frac{7+2\nu_3}{6\nu_3}\right)$$

$$X[6,10] = -(V_1 + V_2)^{-1}\left(\frac{2+2\nu_3}{5-4\nu_3}\right)$$

$$X[7,3] = (V_1 + V_2)^{1/3}$$

$$X[7,4] = (V_1 + V_2)^{-4/3}$$

$$X[7,5] = (V_1 + V_2)$$

$$X[7,6] = (V_1 + V_2)^{-2/3}$$

$$X[7,7] = -(V_1 + V_2)^{1/3}$$

$$X[7,8] = -(V_1 + V_2)^{-4/3}$$

$$X[7,9] = -(V_1 + V_2)$$

$$X[7,10] = -(V_1 + V_2)^{-2/3}$$

$$X[8,3] = \frac{1}{2}(V_1 + V_2)^{1/3}$$

$$X[8,4] = -\frac{1}{3}(V_1 + V_2)^{-4/3}$$

$$X[8,5] = (V_1 + V_2)\left(\frac{7-4\nu_2}{12\nu_2}\right)$$

$$X[8,6] = (V_1 + V_2)^{-2/3}\left(\frac{1-2\nu_2}{5-4\nu_2}\right)$$

$$X[8,7] = -\frac{1}{2}(V_1 + V_2)^{1/3}$$

$$X[8,8] = \frac{1}{3}(V_1 + V_2)^{-4/3}$$

$$X[8,9] = -(V_1 + V_2)\left(\frac{7-4\nu_3}{12\nu_3}\right)$$

$$X[8,10] = -(V_1 + V_2)^{-2/3}\left(\frac{1-2\nu_3}{5-4\nu_3}\right)$$

$$X[9,7] = \frac{5}{2}$$

$$X[9,9] = 1 + 3\left(\frac{7-4\nu_3}{12\nu_3}\right)$$

$$X[9,10] = 1 + 3\left(\frac{1-2\nu_3}{5-4\nu_3}\right)$$

$$X[10,7] = \frac{1}{2}$$

$$X[10,8] = -\frac{1}{3}$$

$$X[10,9] = \left(\frac{7-4\nu_3}{12\nu_3}\right)$$

$$X[10,10] = \left(\frac{1-2\nu_3}{5-4\nu_3}\right)$$

Field Elements of the Submatrixes |*Y|, |*Z**|, and |*T**| are identical to the elements of the submatrix |*X**| with the following modifications: Modifications for the submatrix |*Y**|**

$$Y[9,7] = 0$$

$$Y[9,8] = -\frac{20}{3}$$

$$Y[9,9] = -\frac{1}{2} - \left(\frac{7+2\nu_3}{6\nu_3}\right)$$

$$Y[9,10] = -\left(\frac{10-2\nu_3}{5-4\nu_3}\right) - \left(\frac{2+2\nu_3}{5-4\nu_3}\right)$$

$$Y[10,7] = \frac{5}{2}$$

$$Y[10,8] = 0$$

$$Y[10,9] = 1 + 3\left(\frac{7-4\nu_3}{12\nu_3}\right)$$

$$Y[10,10] = 1 + 3\left(\frac{1-2\nu_3}{5-4\nu_3}\right)$$

Modifications for the Submatrix |*Z|**

$$Z[9,9] = \frac{-1 + 3\left(\frac{7+2\nu_3}{6\nu_3}\right)}{2}$$

$$Z[9,10] = \frac{-2\left(\frac{10-2\nu_3}{5-4\nu_3}\right)+3\left(\frac{2+2\nu_3}{5-4\nu_3}\right)}{2}$$

$$Z[10,7] = 0$$

$$Z[10,8] = \frac{5}{3}$$

$$Z[10,9] = 1-2\left(\frac{7-4\nu_3}{12\nu_3}\right)$$

$$Z[10,10] = 1-2\left(\frac{1-2\nu_3}{5-4\nu_3}\right)$$

Modifications for the Submatrix $|T^*|$

$$T[9,9] = \frac{-1+3\left(\frac{7+2\nu_3}{6\nu_3}\right)}{2}$$

$$T[9,10] = \frac{-2\left(\frac{10-2\nu_3}{5-4\nu_3}\right)+3\left(\frac{2+2\nu_3}{5-4\nu_3}\right)}{2}$$

$$T[10,7] = 1$$

$$T[10,8] = \frac{8}{3}$$

$$T[10,9] = \left(\frac{7+2\nu_3}{6\nu_3}\right)$$

$$T[10,10] = \left(\frac{2+2\nu_3}{5-4\nu_3}\right)$$

References and Notes

(1) Utracki, L. A. In *Polymer Alloys and Blends − Thermodynamics and Rheology*; Hanser Verlag Publishers: Munich, Vienna, New York, 1989.
(2) Gaylord, N. G. in *Copolymers, Polyblends and Composites*; N. A. J. Platzer: Washington, DC, 1975.
(3) Lipatov, Y. S. In *Physical Chemistry of Filled Polymers*; Institute of Polymer Science and Technology: Monograph N°2, British Library: London, 1979.
(4) Dickie, R. A. In *Polymer Blends*; Paul, D. R., Newman, S., Eds.; Vol. 1, Chapter 8, 1978.
(5) Shalaby, S. W. In *Thermal Characterization of polymeric materials*; Turi, E. A., Ed.; Academic Press: London, 1981.
(6) Thomason, J. L. In *Interfaces in Polymer, Ceramic and Metal Matrix Composites*; Ishida, H., Ed.; Elsevier Science: New York, 1988.
(7) Ishida, H.; Koenig, J. L. *Polym. Eng. Sci.* **1978**, *18*, 128.
(8) Kodama, M.; Karino, I. J. *J. Appl. Polym. Sci.* **1986**, *32*, 5345.
(9) Reed, K. E. *Polym. Compos.* **1980**, *1*, 44.
(10) Mijovic, J.; Lin, K. F. *Advances in Chemistry 206*; American Chemical Society: Washington, DC, 1984; Chapter 19.
(11) Douglas, E. P.; Waddon, A. J.; MacKnight, W. J. *Macromolecules* **1994**, *27*, 4344.
(12) Lipatov, Y. S.; Fabulyak, F. G.; Shifrin, V. V. *Polym. Sci. USSR* **1976**, *18*, 866.
(13) Drzal, L. T. *Adv. Polym. Sci. Ser. No. 75* **1986**.
(14) Nielsen, L. E.; Lewis, T. B. *J. Polym. Sci. Polym. Phys. Ed.* **1969**, *7*, 1705.
(15) Eklind, H.; Schantz, S.; Maurer, F. H. J.; Jannasch, P.; Wesslen, B. *Macromolecules* **1996**, *29*, 984.
(16) Eklind, H.; Maurer, F. H. J. *Polymer* **1996**, *37*, 2641.
(17) Eklind, H.; Maurer, F. H. J. *J. Polym. Sci., Phys. Ed.* **1996**, *34*, 1569.
(18) Eklind, H.; Maurer, F. H. J.; Steeman, P. A. M. *Polymer* **1997**, *38*, 1047.
(19) Hammer, C. O.; Maurer, F. H. J. *Polymer* **1998**, *39*, 4243.
(20) Colombini, D.; Martinez-Vega, J. J.; Merle, G.; Girard-Reydet, E.; Pascault, J. P.; Gerard, J. F. *Polymer* **1999**, *40*, 935.
(21) Girard-Reydet, E.; Sautereau, H.; Pascault, J. P. *Polymer* **1999**, *40*, 1677.
(22) Colombini, D.; Merle, G.; Alberola, N. D. *J. Macromol. Sci. − Physics* **1999**, *B38 (5&6)*, 957.
(23) Gregory, B.; Hiltner, A.; Baer, E.; Im, J. *Polym. Eng. Sci.* **1987**, *27(8)*, 568.
(24) Mclaughlin; K. W. *Polym. Eng. Sci.* **1989**, *29(22)*, 1560.
(25) Nazarenko, S.; Haderski, D.; Hiltner, A.; Baer, E. *Polym. Eng. Sci.* **1995**, *35 (21)*, 1682.
(26) Hsieh, A. J.; Guterrez, A. W. *Mater. Res. Soc. Symp.* **1997**, *461*, 165.
(27) Takayanagi, M.; Okamoto, T. *J. Polym. Sci.* **1968**, *23*, 597.
(28) Voigt, V. *Lerchbuch Der Kristall Physik*; Teuber, B. G.: Berlin, 1910.
(29) Reuss, A. *Z. Angweandre Mathematik und Mechanic* **1929**, *49*, 9.
(30) Hashin, Z.; Shtrickman, S. *J. Mech. Phys. Solids* **1963**, *11*, 127.
(31) Hill, R. *J. Mech. Phys. Solids* **1965**, *13*, 213.
(32) Budiansky, B.*J. Mech. Phys. Solids* **1965**, *13*, 223.
(33) Davies, W. E. A. *J. Phys. D* **1971**, *4*, 1176.
(34) Davies, W. E. A. *J. Phys. D* **1971**, *4*, 1325.
(35) Christensen, R. M.; Lo, K. H. *J. Mech. Phys. Solids* **1979**, *27*, 315.
(36) Herve, E.; Zaoui, A. *Int. J. Eng. Sci.* **1993**, *31*, 1.
(37) Colombini, D.; Merle, G.; Alberola, N. D. *Macromolecules* **2001**, *34*, 5916.
(38) Ouali, N.; Cavaille, J. Y.; Perez, J. *J. Plast. Rubber Compos. Process. Appl.* **1991**, *16*, 55.
(39) Alberola, N. D.; Mele, P. *Polym. Compos.* **1996**, *17*, 751.
(40) Eklind, H.; Maurer, F. H. J. *Polym. Networks Blends* **1995**, *5(1)*, 35.
(41) Alberola, N. D.; Merle, G.; Benzarti, K. *Polymer* **1999**, *40*, 315.
(42) Colombini, D.; Merle, G.; Alberola, N. D. *J. Appl. Polym. Sci.* **2000**, *76*, 530.
(43) Colombini, D.; Merle, G.; Alberola, N. D. *Macromol. Symp.* **2001**, *169*, 235.
(44) Dickie, R. A. *J. Appl. Polym. Sci.* **1973**, *17*, 45.
(45) Maurer, F. H. J. In *Polymer Composites*; Sedlacek, B., Ed.; W. de Gruyter & Co.: Berlin, 1986; p 399.
(46) Maurer, F. H. J. In *Controlled Interphases in Composite Materials*; Ishida, H., Ed.; Elsevier Science: New York, 1990; p 491.
(47) Van der Poel, C. *Rheol. Acta* **1958**, *1*, 189.
(48) Frohlich, J.; Sack, R. *Proc. R. Soc.* **1946**, *A165*, 415.
(49) Bohn, L. *Adv. Chem. Ser.* **1974**, *142*, 66.
(50) Neyertz, S.; Brown, D.; Colombini, D.; Alberola, N. D.; Merle, G. *Macromolecules* **2000**, *33*, 1361.
(51) Booij, H. C.; Thoone, G. P. J. M. *Rheol. Acta* **1982**, *21*, 15.

MA020266L